THE JOURNAL OF BIOLOGICAL CHEMISTRY VOL. 291, NO. 53, pp. 27007–27022, December 30, 2016

Phaseic Acid, an Endogenous and Reversible Inhibitor of Glutamate Receptors in Mouse Brain*

Received for publication, August 31, 2016, and in revised form, November 18, 2016 Published, JBC Papers in Press, November 18, 2016, DOI 10.1074/jbc.M116.756429

Sheng Tao Hou[‡§¶1], **Susan X. Jiang**[§], **L. Irina Zaharia**[‖], **Xiumei Han**[‖], **Chantel L. Benson**[‖], **Jacqueline Slinn**[§], **and Suzanne R. Abrams**[‖2]

From the [‡]*Brain Research Centre and Department of Biology, Southern University of Science and Technology, 1088 Xueyuan Boulevard, Nanshan District, Shenzhen, 518055 Guangdong Province, China,* [§]*Experimental NeuroTherapeutics, Human Health Therapeutics Portfolio, National Research Council Canada, 1200 Montreal Road, Building M54, Ottawa K1A 0R6, Ontario, Canada,* [‖]*Aquatic and Crop Resource Development, National Research Council Canada, 110 Gymnasium Place, Saskatoon, Saskatchewan S7N 0W9, Canada, and the* [¶]*Department of Biochemistry, Microbiology and Immunology, Faculty of Medicine, University of Ottawa, Ontario K1H 8M5, Canada*

Edited by F. Anne Stephenson

Phaseic acid (PA) is a phytohormone regulating important physiological functions in higher plants. Here, we show the presence of naturally occurring (−)-PA in mouse and rat brains. (−)-PA is exclusively present in the choroid plexus and the cerebral vascular endothelial cells. Purified (−)-PA has no toxicity and protects cultured cortical neurons against glutamate toxicity through reversible inhibition of glutamate receptors. Focal occlusion of the middle cerebral artery elicited a significant induction in (−)-PA expression in the cerebrospinal fluid but not in the peripheral blood. Importantly, (−)-PA induction only occurred in the penumbra area, indicting a protective role of PA in the brain. Indeed, elevating the (−)-PA level in the brain reduced ischemic brain injury, whereas reducing the (−)-PA level using a monoclonal antibody against (−)-PA increased ischemic injury. Collectively, these studies showed for the first time that (−)-PA is an endogenous neuroprotective molecule capable of reversibly inhibiting glutamate receptors during ischemic brain injury.

Phaseic acid (PA),[3] a terpenoid catabolite of abscisic acid (ABA), is generated spontaneously after 8′-hydroxylation of ABA by cytochrome P-450s in the CYP707A subfamily (1). In higher plants, PA and ABA act as phytohormones regulating important physiological functions in growth and development as well as in responses to biotic and abiotic stress (cold, drought, heat exposure, and salinity). The regulation of these processes is mediated by a change in endogenous PA and ABA levels that are controlled by the balance between biosynthesis and metabolism. ABA induces the production of the second messenger cyclic ADP-ribose, which controls the release of stored intracellular calcium in plants to exert its effect (2–4).

ABA in plants can be metabolized by conjugation and oxidation. The principal oxidative pathway of natural (+)-ABA, mediated by cytochrome P-450 monooxygenases, occurs through hydroxylation of the 8′-methyl group, resulting in 8′-hydroxy-ABA, which rearranges to (−)-PA (1). Further enzymatic reduction of (−)-PA leads to the production of DPA. Similar to ABA, naturally occurring (−)-PA is a plant hormone associated with photosynthesis arrest and abscission (5). However, very little is known about the presence and function of PA in the mammalian system.

Stroke is a leading cause of death and disability in the world. However, lack of protective methods against stroke-induced brain injury still represents one of the largest unmet medical needs (6, 7). Despite decades of effort trying to find ways to protect neurons against ischemic insult, no clinically effective drugs are available. It is known that the brain can indeed launch an internal protective response against ischemic insult, such as activating autophagy machinery (8). However, in general, the brain's endogenous protective mechanisms against cerebral ischemia remain not well understood. Further understating of the internal defense system would be extremely beneficial to develop appropriate drugs against stroke in humans.

Cerebral ischemia induces rapid neuronal cell membrane depolarization and activates NMDA-type glutamate receptors (NMDARs). Subsequent increased calcium influx through NMDARs causes excitotoxicity, a process that is toxic to neurons and contributes to a wide range of neurological disorders, such as cerebral ischemia (6, 9, 10). Although drugs directly blocking NMDARs are effective in neuroprotection, all have failed to be approved for clinical use due to their severe side

* This work was supported by National Natural Science Foundation of China Grant 81571287, Shenzhen Science and Technology Innovation Committee Basic Science Research Grants JCYJ20140417105742709 and JCYJ20160301112230218, State Key Laboratory of Neuroscience Open Competition Grant SKLN-201403, Southern University of Science and Technology (SUSTech) Peacock Program Start-up Fund Grant 22/Y01226109, and SUSTech Brain Research Centre Fund (to S. T. H.). The authors declare that they have no conflicts of interest with the contents of this article.

[1] To whom correspondence should be addressed: Brain Research Centre and Dept. of Biology, Southern University of Science and Technology, 1088 Xueyuan Blvd., Nanshan District, Shenzhen, 518055 Guangdong Province, China. Tel.: 86-755-8801-8418; E-mail: hou.st@sustc.edu.cn.

[2] Present address: Saskatchewan Structural Sciences Centre, Rm. 190 Thorvaldson Bldg., 110 Science Place, University of Saskatchewan, Saskatoon, Saskatchewan S7N 5C9, Canada.

[3] The abbreviations used are: PA, phaseic acid; ABA, abscisic acid; DPA, dihydrophaseic acid; ABA-GE, abscisic acid glucose ester; DW, dry sample weight; CSF, cerebrospinal fluid; MCAO, middle cerebral artery occlusion; TTC, 2,3,5-triphenyltetrazolium chloride; UPLC, ultraperformance liquid chromatography; NMDAR, NMDA-type glutamate receptor; TTR, transthyretin; PDGFR, PDGF receptor; GFAP, glial fibrillary acidic protein; Ab, antibody; QC, quality control; PSS, physiological saline solution; HBSS, Hanks' balanced salt solution; ANOVA, analysis of variance.

effects affecting normal physiological functions of NMDARs. It has been suggested that compounds with properties to reversibly and uncompetitively block NMDARs are the preferred candidates for development as therapeutics against stroke (9).

Because ABA is known to modulate the release of intracellularly stored calcium to affect plant guard cell death (3, 11–13), we were intrigued as to whether ABA and its metabolites might be involved in animal neuronal calcium homeostasis and regulation. In particular, the presence of ABA has been shown in the brains of pigs and rats (11), and therefore it is highly possible that the surge in intracellular calcium following cerebral ischemia in the ischemic core in the brain can be affected by the presence of ABA and its metabolites. However, our data showed the presence of surprisingly high levels of endogenous (−)-PA, but not other ABAs, in the choroid plexus, CSF, and vascular endothelial cells in the ischemic mouse and rat brains. The localization of (−)-PA was only in the penumbra area surrounding the ischemic infarct core, indicating its involvement in neuroprotection. Interestingly, (−)-PA reversibly inhibits glutamate receptors, reduces intracellular calcium influx, and protects cortical neurons against glutamate toxicity *in vitro* and *in vivo*. These studies revealed a previously unknown role of PA serving as an endogenous mechanism of neuroprotection in ischemic brain and suggest that (−)-PA or its analogous can be developed as a powerful agent for neuroprotection against stroke.

Results

The Presence of (−)-PA in Mouse and Rat Brains—We have successfully developed methods to analyze and quantify PA and its metabolites in mouse and rat brain tissues. Using ultra performance liquid chromatography coupled with tandem mass spectrometry (UPLC/MS/MS), deuterium-labeled internal standards were used and spiked in samples to confirm the identity of PA species (Fig. 1). Levels of PA, DPA, ABA, 7′-OH-ABA, *neo*-PA, ABA-GE, and *trans*-ABA from both mouse brain and blood were accurately measured and quantified against dry sample weight (DW) using UPLC/MS/MS (Fig. 2).

To determine the stereochemical nature of the observed PA, tissue samples were chromatographed using a chiral column, and the identity of the observed PA was checked against synthetic standards of the natural form of PA: (−)-PA and the unnatural mirror image form of PA, (+)-PA (Fig. 1, *A* and *B*). Near baseline enantioseparation of PA in standard solutions was achieved by a gradient elution mode as described under "Experimental Procedures." The chromatograms of PA in mouse brain tissue and blood samples were compared with that of the known standards. Spiking experiments of brain and blood samples with known amounts of natural (−)-PA standard resulted in the corresponding increase of PA signal in the mouse brain tissue and mouse blood. confirming the same stereochemistry as the plant-derived compound. The chromatograms of (−)-PA in rat brain tissue, CSF, and blood samples were also compared with that of the known standards. Spiking experiments of rat CSF, blood, and samples with known amounts of natural (−)-PA standard also resulted in the corresponding increase of the PA signal in the rat CSF, blood, and brain, confirming the same stereochemistry as the plant-derived compound (Fig. 1*D*). Based on the spiking experiment using the two forms of PA standards shown in Fig. 1, *B–D*, it is clear that mouse and rat brains, CSF, and blood contain only (−)-PA, the naturally occurring form of PA.

Mouse brain contains a small amount of ABA (74.9 ± 45.2 ng/g DW; $n = 12$), which was in agreement with an earlier report on the presence of ABA in pig and rat brains (14). However, the brain ABA level was almost 30 times lower than that of (−)-PA (2245.20 ± 573.20 ng/g DW; $n = 15$) (Fig. 2*A*). A high level of (−)-PA was consistently detected in both the right and left hemispheres of the brain. Mouse blood does contain (−)-PA, but the level was 10-fold lower compared with that found in the brain tissue (232.20 ± 90.68 ng/g DW; $n = 4$; as shown in Fig. 2*A*, $p > 0.01$, paired *t* test). All other ABA metabolites were also present in extremely low quantities in the blood of mouse fed with standard diet.

(−)-PA Is Endogenously Produced in the Brain—To determine the source of mouse brain (−)-PA, we tested the content of ABA derivatives in mouse food pellet. Mouse food with fixed ingredients was obtained from a commercial source. As shown in Fig. 2*B*, standard mouse food pellet contains very low levels of ABA and PA. Analysis of the food pellets showed the presence of low amounts of DPA (341 ng/g DW), PA (27 ng/g DW), ABA (42 ng/g DW), *neo*-PA (36 ng/g DW), and *trans*-ABA (47 ng/g DW) (Fig. 2*B*). This result argues against the assumption that brain (−)-PA might be the result of accumulation of ABA from food sources.

Moreover, to determine whether food-borne ABA can even be converted to (−)-PA and accumulated in the brain, mice were injected i.v. with purified (+)-ABA and (−)-ABA at 45 or 112.5 mg/kg each (Fig. 2*C*). These high amounts of ABA were arbitrarily used to detect a surge of their derivatives in the brain. Ethanol (2%) or saline, used as a solvent for ABA, was also injected in the mouse to serve as a control. No clear increase in PA or DPA occurred in mouse brain tissue. Only inductions of (+)-ABA and ABA-GE were observed in mouse brain after 2 h of injection of ABA. Both (+)-ABA and ABA-GE were decreased significantly after 5 h of injection into the brain, indicating that the high level of (−)-PA occurring in mouse brain was in fact produced endogenously in the brain. Together, these data support the fact that brain (−)-PA could not have been derived from external sources.

The Presence of (−)-PA in CSF, Choroid Plexus, and Cerebral Vascular Endothelial Cells—To demonstrate the exact location of (−)-PA in the brain, a mouse monoclonal antibody specific to PA was used (15). This antibody cross-reacts with both forms of PA but does not react with ABA or DPA (15). Because UPLC/MS/MS data showed the presence of only (−)-PA in mouse and rat brain tissues and the blood, it was assumed that PA antibody reactivity would represent reactivity to (−)-PA in the brain. The specificity of the PA antibody to mouse brain tissue was confirmed using an immunosorbent assay to remove the primary or secondary antibody yielding negative staining on an indirect immunofluorescence assay (not shown). Strong PA immunofluorescence was detected in the choroid plexus (Fig. 3, *A–C*) and on the cerebral vascular walls (Fig. 3, *D–J*). Double immunostaining with antibodies specific to choroid plexus cells (TTR) and PA confirmed co-localization of PA with choroid

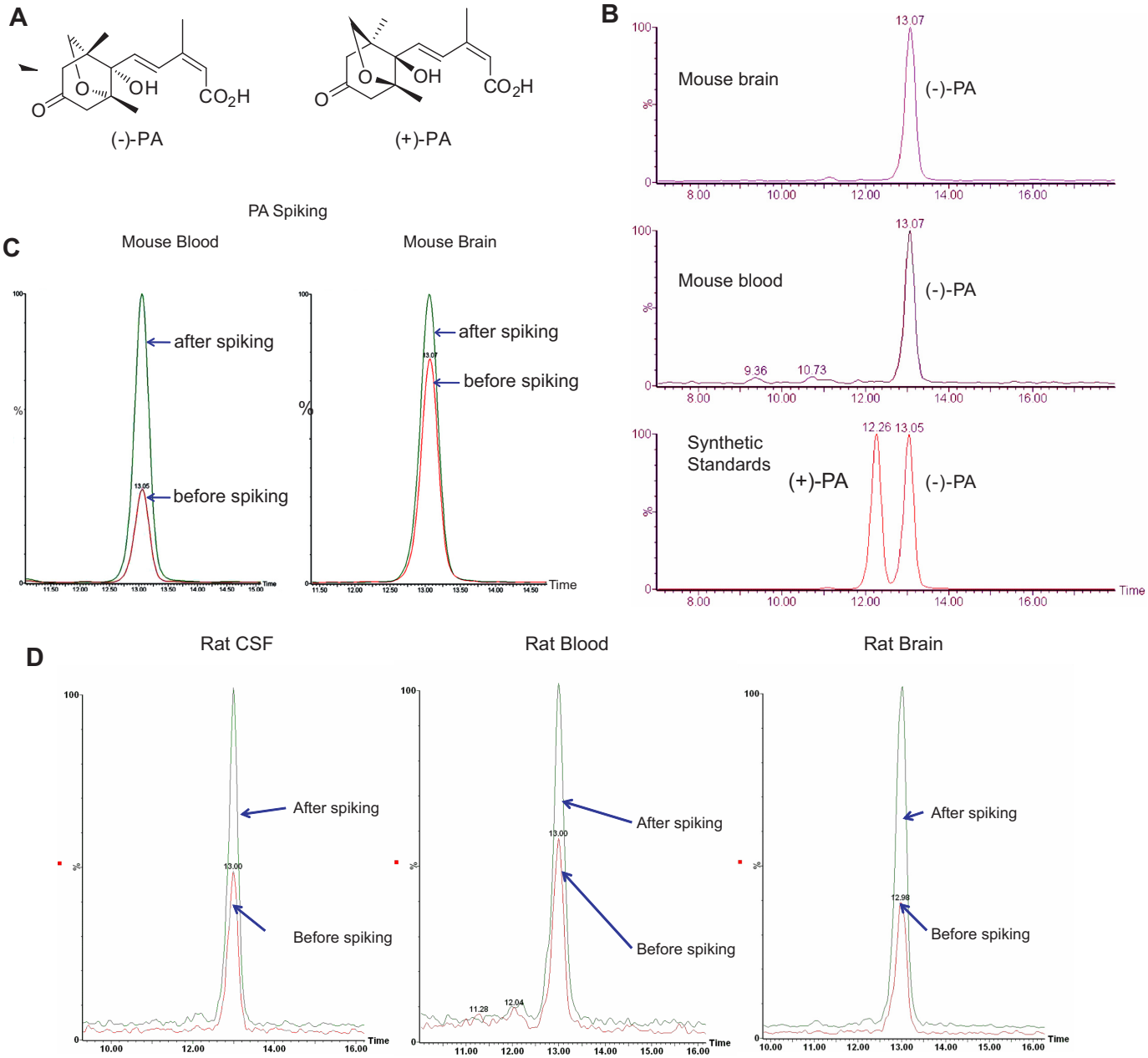

FIGURE 1. **Identification and characterization of PA in rodent brains.** Chemical structures of (+)-PA and (−)-PA are shown in *A*. Near baseline enantioseparation of PA in standard solutions was achieved by a gradient elution mode as described under "Experimental Procedures." Brain and blood samples were subjected to UPLC/MS/MS using a chiral column and then compared with known standards shown in *B*. Spiking experiments of brain and blood samples with known amounts of standards were also performed to confirm that only naturally occurring (−)-PA was present in mouse (*B* and *C*) and rat (*D*) tissues.

plexus epithelial cells (Fig. 3, *B* and *B′*). Higher magnification of the choroid plexus immunostaining showed that PA appeared in the cytoplasm of all cells lining the choroid plexus. Furthermore, PA double immunostaining showed positive co-localization of PA with CD31 and lectin (Fig. 3, *D–I*), but not PDGFRβ, GFAP, NeuN, and IBA-1 (Fig. 3, *J–M*), indicating that PA was endogenously produced in the brain by choroid plexus and vascular endothelial cells.

Cerebral Ischemia Induces (−)-PA Production in the CSF and Ischemic Penumbra—To determine the function of (−)-PA in the brain, mouse and rat middle cerebral artery occlusion (MCAO) models were used in the study (Fig. 4*A*). MCAO elicited a significant increase in the level of (−)-PA after 2 h of reperfusion in the ischemic mouse brain (Fig. 4*B*). The (−)-PA level reached its peak at 24 h of reperfusion and gradually decreased in both cortices to basal level after 28 days of reperfusion (Fig. 4*B*).

The presence of (−)-PA in rat ischemic brain (Fig. 4*C*) and in rat CSF (Fig. 4*D*), but not in rat peripheral blood (Fig. 4*D*), also increased significantly after 24 h of reperfusion. Because of technical difficulties in obtaining adequate quantities of CSF from the mouse brain, only rat CSF was collected and quantified using UPLC/MS/MS. As shown in Fig. 4*D*, rat CSF contains a level of (−)-PA comparable with that found in the brain but a significantly higher level of (−)-PA compared with that in the blood (Fig. 4*D*). Together, it is very interesting that MCAO

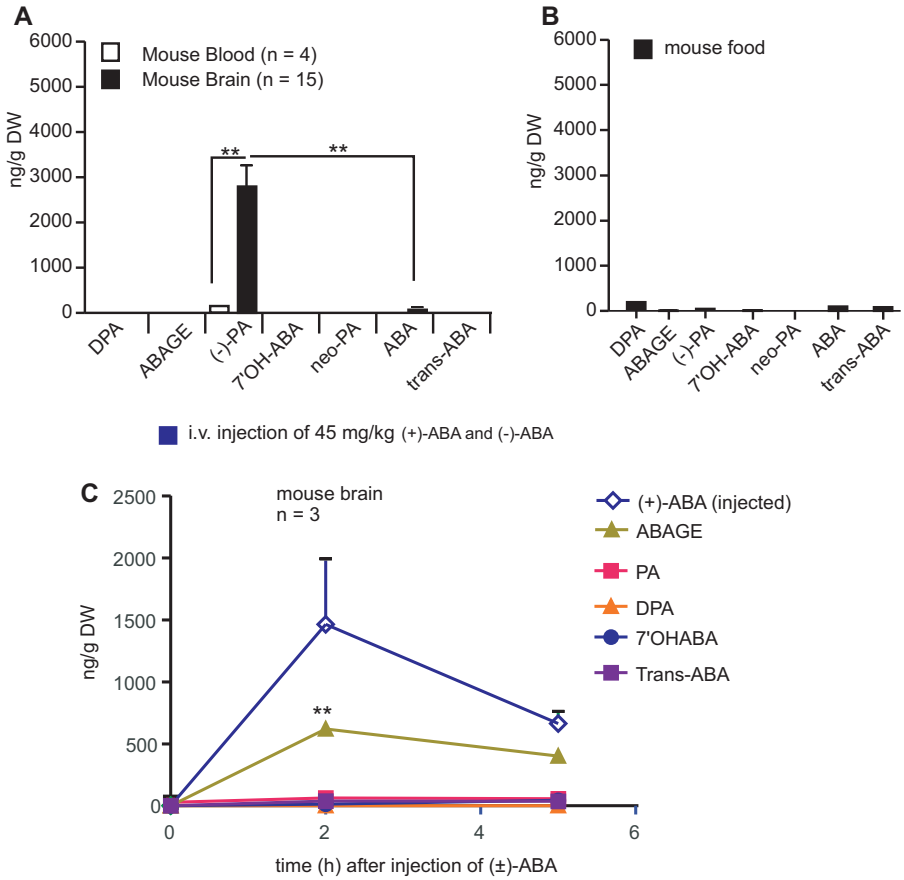

FIGURE 2. **(−)-PA is endogenously produced in the brain.** Mouse brain tissue, blood, and mouse food pellets were collected, freeze-dried, and subjected to UPLC/MS/MS as described under "Experimental Procedures." PA, ABA, and its metabolites from mouse brain tissue (*A*), blood (*A*), and mouse food pellets (*B*) were quantitatively determined against DW. ** indicates statistical significance ($p < 0.01$ by paired *t* test; $n = 4$ for blood; $n = 15$ for brain tissues). Both (+)-ABA and (−)-ABA at a dose of 45 mg/kg each were injected into mouse veins. After 2 and 5 h, brains were collected to determine the level of PA and other ABA metabolites in the brain as shown in *C*. *Error bars* represent the mean ± S.E. ** indicates statistical significance ($p < 0.01$ by paired *t* test; $n = 3$).

treatment induced (−)-PA expression in both the contralateral and ischemic sides of the brain, indicating that (−)-PA might play a protective role in the ischemic brain.

To establish the exact location of (−)-PA in the ischemic mouse brain, double immunohistochemical staining for PA was performed (Fig. 5). PA immunofluorescence increased dramatically in the penumbra area (Fig. 5, *A* and *F*, *area 3*) compared with the ischemic infarct core area (Fig. 5, *A* and *E*, *area 2*) and the sham-operated mouse brain (Fig. 5, *C* and *J*). Using tissue laser capture microdissection techniques, we collected brain tissues from the ischemic core (Fig. 5*A*, *area 2*), the penumbra (Fig. 5*A*, *area 3*), the contralateral side (Fig. 5*A*, *area 4*), and the sham brain for UPLC/MS/MS analysis. The result showed that the (−)-PA level was significantly higher in the penumbra and the contralateral side of the brain than that in the ischemic core (Fig. 5*J*). Cerebral vascular localization of PA was also much pronounced in the penumbra area (Fig. 5, *G–I*) based on double immunostaining. These studies indicated that the naturally occurring (−)-PA may play an important role in the ischemic brain.

(−)-PA Reversibly Inhibits Glutamate Receptors—Glutamate-mediated excitotoxicity plays a major role in ischemic neuronal injury (6, 7). Chemical compounds that reversibly inhibit glutamate receptors can protect brain from ischemic damage (9, 10). Experiments were therefore designed to determine whether (−)-PA has any effect on cortical glutamate receptors. Based on results derived from the following two experiments, it is clear that (−)-PA functions as a reversible glutamate receptor inhibitor.

First, a ratiometric calcium assay using Fura2-AM showed that (−)-PA dose-dependently inhibited cortical neuronal intracellular calcium ($[Ca^{2+}]_i$) influx when treated with 100 μM NMDA (Fig. 6, *A* and *B*). (−)-PA alone ranging from 10 to 1000 μM did not affect neuronal $[Ca^{2+}]_i$ but effectively reduced the NMDA-induced increase in $[Ca^{2+}]_i$. Interestingly, inhibition of $[Ca^{2+}]_i$ by (−)-PA was reversible, and the effect of (−)-PA can be washed off using culture medium. Subsequently, neurons showed a strong surge of $[Ca^{2+}]_i$ in response to KCl depolarization, which served as a control (Fig. 6*A*). The -fold reduction of $[Ca^{2+}]_i$ by (−)-PA was quantified from measurements of at least 20 cells, and the results are shown in Fig. 6*B*. These observations suggested that (−)-PA is a potential reversible inhibitor of glutamate receptors.

Second, whole-cell patch clamp recordings demonstrated a dose-dependent inhibition of NMDA-activated currents by (−)-PA (Fig. 6, *C*, *D*, and *E*). The effect of (−)-PA and NMDA on neuronal excitability was first determined in cultured cortical neurons. As shown in Fig. 6*C*, 50 μM NMDA plus 1 μM glycine induced a large inward current at −50 mV. In contrast, application of (−)-PA with a series of concentrations ranging

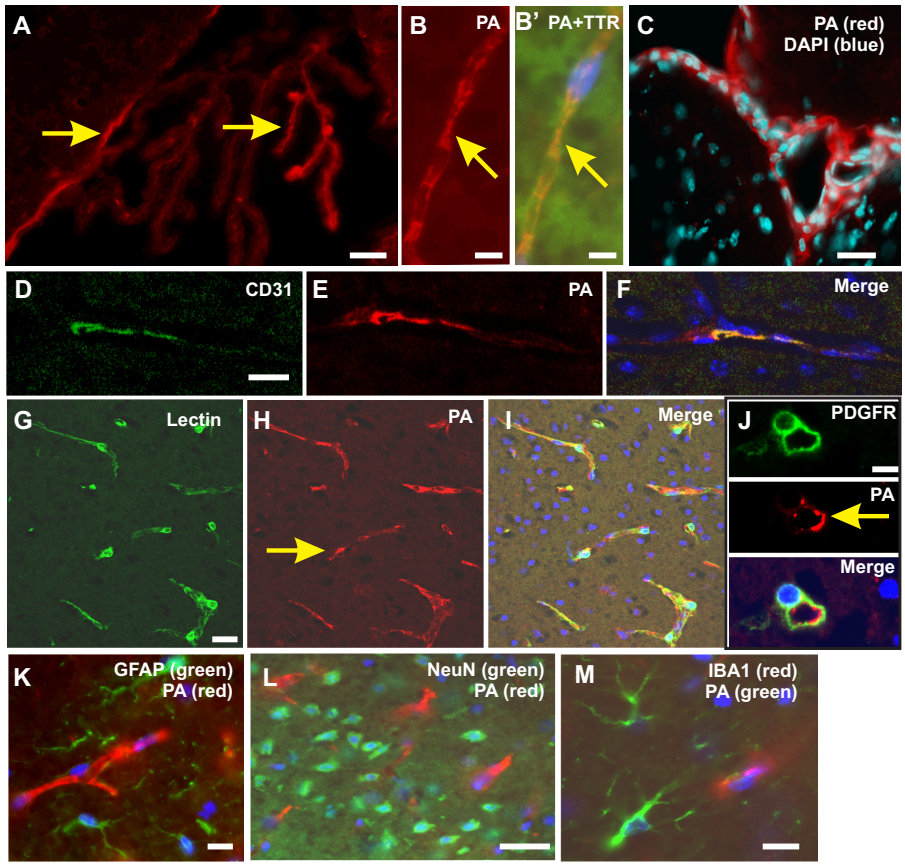

FIGURE 3. **The presence of PA in the choroid plexus and vascular endothelial cells.** Immunofluorescence staining with a monoclonal antibody to PA under a confocal microscope showed a clear PA positivity in the choroid plexus in the cerebral ventricles (*red* color; *arrows* in *A* and *B*). Double immunofluorescence staining of PA (*B*; *red* color) with TTR (*B'*; *green* color) showed PA co-localization with TTR (*yellow* color in merged image in *B'*). Double immunostaining of PA (*red color* in *C*, *E*, *F*, *H*, *I*, *J*, *K*, and *L*) with DAPI (*C*; *blue* color), CD31 (*D*; *green* color), lectin (*G*; *green* color), PDGFRβ (*J*; *green* color), GFAP (*K*; *green* color), NeuN (*L*; *green* color), and microglia (*M*; *red* color) was also performed to show co-localization. PA immunostaining was co-localized with CD31 (*F; yellow color*) and lectin staining (*I; yellow color*), indicating that PA is expressed by endothelial cells. PA did not show co-localization with pericytes (*J; bottom panel*), which surround the microvessels, or with astrocytes (*K*), microglia (*M*), and neurons (*L*). *Scale bars*, 50 μm.

between 10 and 1000 μM neither induced any detectable current at −50 mV nor affected the membrane potential (not shown). To determine the effect of (−)-PA on NMDA-activated current, the dose-response relationship was established by application of NMDA for 30 s followed by addition of (−)-PA (Fig. 6, *C* and *D*). (−)-PA inhibited NMDA-activated current in a dose-dependent manner (Fig. 6*E*) over the range between 100 and 1000 μM with an IC_{50} of 34.37 ± 0.012 μM and a Hill slope factor of 1.712 ± 0.038 (n = 10). This inhibition was fully reversible after a few seconds of washing. Results from these experiments showed that (−)-PA not only dose-dependently but also in a reversible manner inhibited NMDA current. When (−)-PA and NMDA were removed, the membrane potential fully returned to the normal resting level. Collectively, these experiments demonstrated that (−)-PA reversibly and transiently blocks glutamate receptors and potentially plays a key role in preventing excitotoxicity in the ischemic brain.

(−)-PA Protects Cortical Neurons against Glutamate Toxicity—Cultured cortical neurons underwent cell death in response to bath incubation with NMDA at 100 μM for 6 h (Fig. 7*A*). Pretreatment of neurons with (−)-PA inhibited neuronal death dose-dependently against NMDA toxicity (Fig. 7*B*). Both phase-contrast and DAPI staining images are shown in Fig. 7*C*. (−)-PA itself has no toxicity to cultured neurons (Fig. 7*A*). A calpain inhibitor, *N*-acetyl-L-leucyl-L-leucyl-L-norleucinal, was a very effective neuroprotectant against NMDA toxicity to neurons (Fig. 7*B*), which served as a positive control.

Elevation of (−)-PA Level Reduced Ischemic Brain Injury—To determine whether (−)-PA was indeed protective against cerebral ischemia, (−)-PA was delivered to the mouse brain using a preimplanted osmotic pump through a cannula to the left cerebral ventricle on the ischemic side of the brain. Mice treated with (−)-PA and vehicle had a similar survival rate as this particular MCAO mouse model has a very low mortality rate over the period of surgery and recovery (Fig. 7*D*). Mice receiving (−)-PA showed no change in survival rate compared with the vehicle-treated group serving as a control. However, the ischemic infarct size was significantly reduced in the (−)-PA-treated group after 24 days of reperfusion (Fig. 7*E*). Furthermore, (−)-PA-treated mice showed significantly better improvement in neurological deficit scores compared with the MCAO mice treated with vehicle (MCAO-vehicle group) after 6 and 24 days of reperfusion (Fig. 7*F*). These results indicated that (−)-PA is neuroprotective.

Reduction in (−)-PA Level in the Brain Worsens MCAO Outcomes—Monoclonal antibody against PA was delivered to the brain left ventricle just before MCAO using a preimplanted osmotic pump through a cannula to the left cerebral ventricle

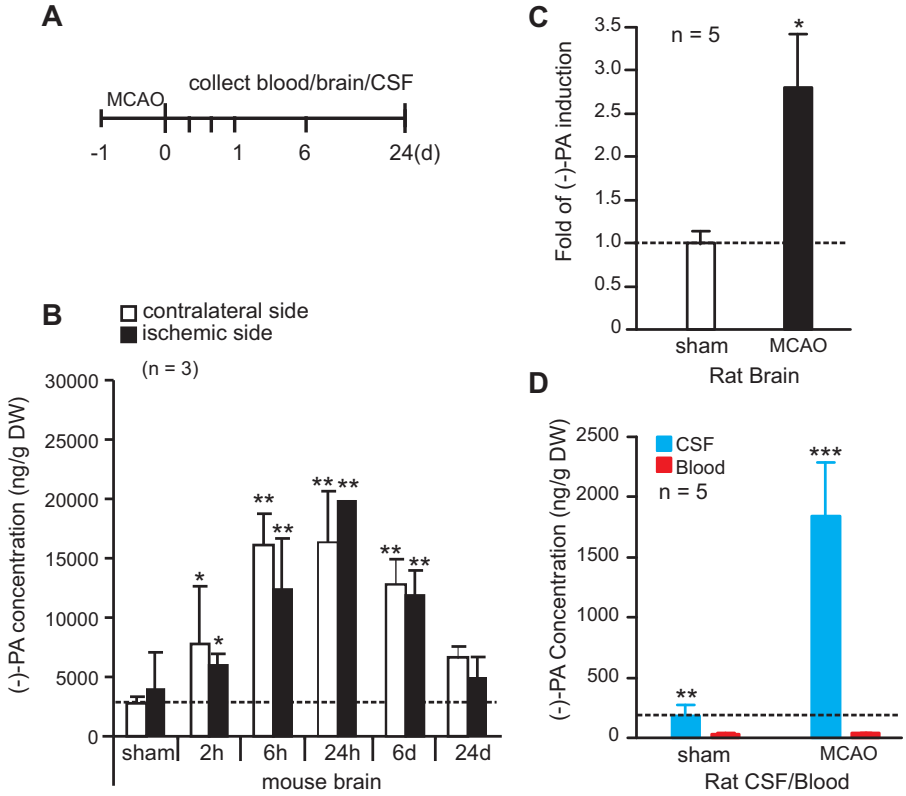

FIGURE 4. **Cerebral ischemia elevates the level of (−)-PA in the CSF and brain.** *A*, schematic diagram of MCAO model. The middle cerebral artery was occluded for 1 h and followed by up to 24 days of reperfusion. Blood and brain tissues were collected at 2 h, 6 h, 24 h, 6 days, and 24 days after reperfusion. CSF was collected after 24 h of reperfusion. Samples were subjected to UPLC/MS/MS analysis. *B* shows the elevated (−)-PA level in both the ipsilateral and contralateral sides of the ischemic brain. Rat brains were collected after 24 h of reperfusion, and -fold induction of (−)-PA was determined and is presented in *C*. CSF and blood were taken after 24 h of reperfusion from MCAO rats, and the concentration changes are shown in *D*. *Error bars* represent the mean ± S.D. * indicates $p < 0.05$, ** indicates $p < 0.01$, and *** indicates $p < 0.001$ (one-way ANOVA with Tukey's post hoc analysis; $n = 5$). *d*, days.

on the ischemic side of the brain. After 24 days of reperfusion, 2,3,5-triphenyltetrazolium chloride (TTC) staining of the ischemic brain showed a much enlarged ischemic infarct core compared with the vehicle-treated group (Fig. 8, *A* and *B*). Indeed, the PA antibody-treated group (MCAO + PA Ab) exhibited significant deterioration of neurological deficit scores (Fig. 8*C*) and reduced forepaw pulling strength (Fig. 8*D*) compared with the MCAO-only group (MCAO − PA Ab group) following MCAO, indicating that reduced PA expression in the brain worsens neurological outcomes of cerebral ischemia. Treatment of mice with PA Ab, without MCAO, had no effect on the survival rate, neurological scores, or brain tissue damage, which served as a control.

To confirm the level of (−)-PA in the brain after antibody treatment, immunostaining was performed to demonstrate the reduction of PA expression levels in both the ischemic infarct core tissue (Fig. 8, *E* and *F*) and the penumbral tissue (Fig. 8, *E* and *G*). For comparison with a control group without PA antibody treatment, please see Fig. 5, *D*, *E*, and *F*. Tissue microdissection was used to isolate brain tissue from these areas. Samples were subjected to UPLC/MS/MS analysis (Fig. 8*H*). Indeed, infusion of PA antibody to the brain inhibited the rise of the (−)-PA level in the ischemic mouse brain.

Discussion

In the present study, we profiled the presence of plant stress hormone PA and all major ABA metabolites in mouse and rat brains. Except for (−)-PA, no other plant ABA metabolites appear to be present in quantifiable amounts in mouse and rat brain and blood. (−)-PA occurs in high quantities in rodent brain tissues relative to a much lower level of (−)-PA in the peripheral blood. Cerebral ischemia evoked a significant increase in (−)-PA in the ischemic brain penumbra, particularly in the CSF, compared with the sham-operated animals. Brain (−)-PA was from endogenous sources (cerebral endothelial cells and the choroid plexus) rather than exogenous sources (such as accumulation from the food). Importantly, endogenously produced (−)-PA plays a role in reversibly blocking glutamate receptors during cerebral ischemia in tissues surrounding the ischemic core, suggesting that naturally occurring (−)-PA is an endogenous neuroprotectant of the brain. To the best of our knowledge, this is the first report of the presence of (−)-PA in rodent brains. There is no prior information about the mechanism of PA action in animals. It is therefore intriguing to see the presence of a high level of (−)-PA in the CSF of ischemic brains, which may represent an internal defense system during brain injury. The utility of these findings warrants further investigation.

Is brain (−)-PA derived from ABA metabolism? ABA in plants can be metabolized by conjugation and oxidation. The principal oxidative pathway of natural (+)-ABA is mediated by cytochrome P-450 monooxygenases (Fig. 9, **1**) (1) through hydroxylation of the 8′-methyl group. The resulting 8′-hydroxy-

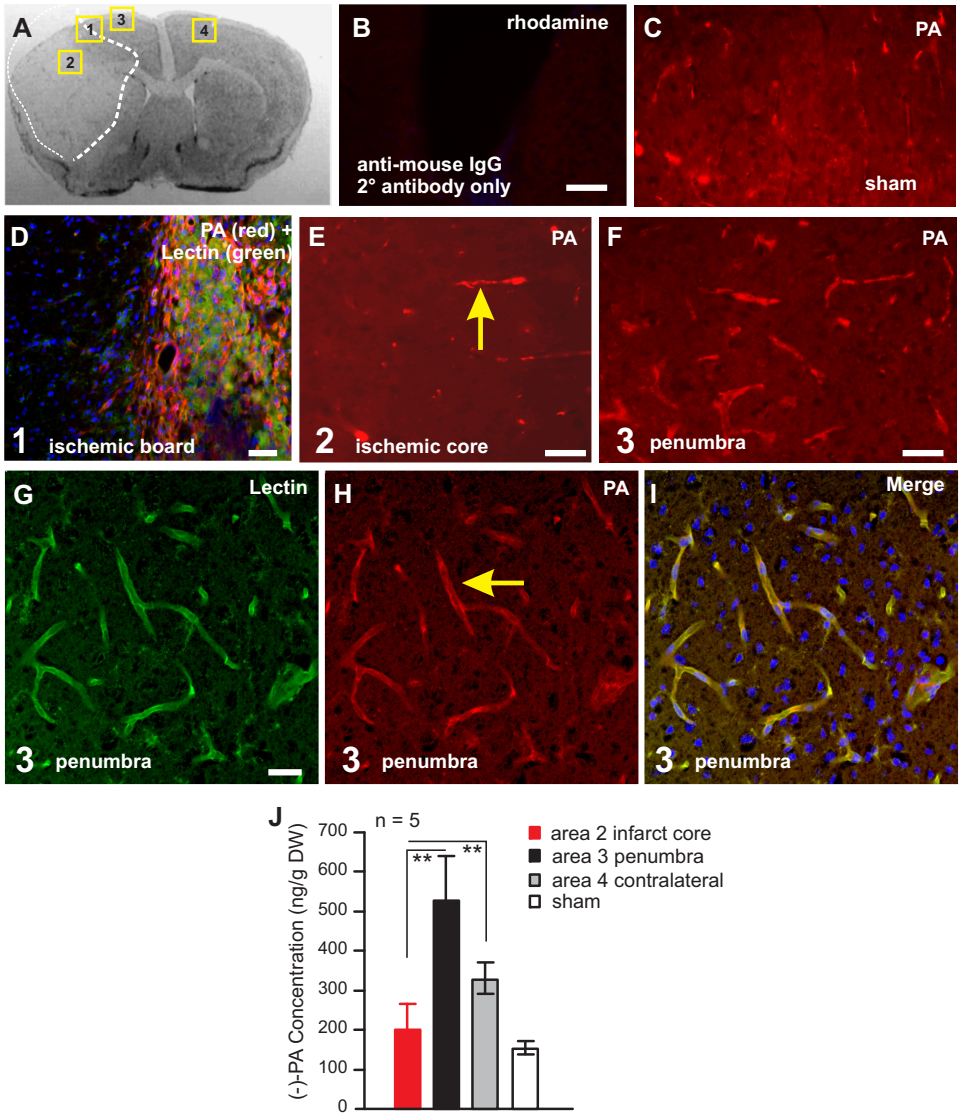

FIGURE 5. **MCAO elevated (−)-PA level in the non-ischemic tissue.** An example of a coronal section of the ischemic brain is shown in *A*. *Numbers 1–4* in the *squares* in *A* indicates areas of interest. PA immunostaining omitting the primary antibody was performed to show tissue specificity (*B*). The expression of PA in sham-operated mouse brain (*C*) and ischemic brain (*D–I*) were examined under a fluorescence microscope. Lectin was labeled as *green* fluorescence in *D* and *G*. Co-localization of lectin with PA is shown in *I*. Laser capture microdissection was used to obtain tissues from areas of interests as indicated in *A*. These samples were subjected to UPLC/MS/MS analysis to detect (−)-PA levels as shown in *J*. *Error bars* represent the mean ± S.E. ** indicates $p < 0.05$ compared with *area 2* of tissues from the infarct core (one-way ANOVA with Tukey's post hoc analysis; $n = 5$). *Scale bars*, 50 μm.

ABA can be rearranged to PA. Further enzymatic reduction of PA leads to DPA (Fig. 9, **4**). Other metabolic steps (for reviews, see Refs. 16 and 17) include hydroxylation of the 7′- and 9′-methyl groups of the ABA ring as well as conjugation of glucose esters (ABA-GE). *trans*-ABA is a product of isomerization of natural ABA under UV light. In plants, the unnatural mirror image form, (−)-ABA, is mainly metabolized by hydroxylation at the 7′-methyl group, but there are also reports of the unnatural mirror image form of PA (Fig. 9, **7**) as a minor product resulting from the feeding of unnatural (−)-ABA to maize cell suspension culture (18).

Although it is not possible to fully rule out an external source of (−)-PA as we still do not have any direct proof of local production, based on the current study, it is highly unlikely that the high level of naturally occurring (−)-PA was the result of ABA metabolism in the brain. First, both mouse and rat brains and their blood contain very low levels of ABA and its intermediates. Even injection of large quantities of (+)-ABA and (−)-ABA into the blood stream failed to produce a noticeable increase in (−)-PA level. Second, the (−)-PA level in the brain was close to 2500 times higher than that of ABA, whereas the ABA levels in mouse and rat tissues were almost undetectable. This makes it inconceivable for such a low amount of ABA to be transformed into the high level of (−)-PA. Third, mouse food has an extremely low level of ABA and an almost undetectable amount of (−)-PA, confirming a previous report by Le Page-Degivry *et al.* (14) that showed that the low level of ABA contents of rat brain tissue was not correlated with the amount of ABA in the diet as animals fed for two generations on a synthetic ABA-poor diet had more ABA in their brains than control animals. We show here that, apart from very low levels of DPA and trace amounts of ABA and *trans*-ABA, no other ABA

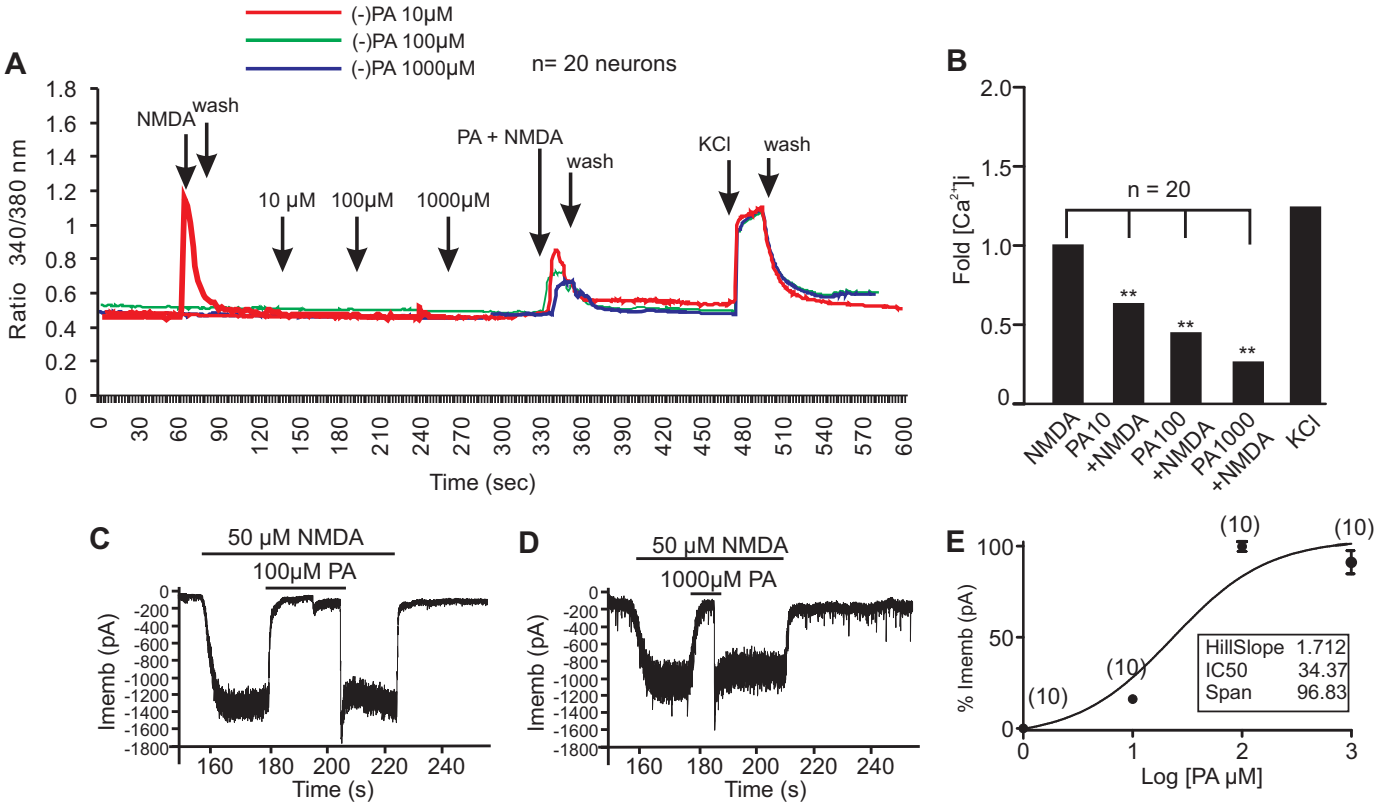

FIGURE 6. **Reversible inhibition of NMDA receptors by (−)-PA.** *A*, ratiometric calcium imaging. Cultured cortical neurons on glass coverslips were loaded with Fura-2 AM for 30 min followed by washing with PSS or HBSS buffer. (−)-PA at the indicated concentrations was added to neurons. Fura-2 fluorescence from more than 10 selected neurons was measured for up to 30 min. After washing with PSS or HBSS buffer, NMDA with or without (−)-PA at the indicated dosage was loaded onto neurons. Addition of KCl showed a large $[Ca^{2+}]_i$, confirming that these neurons were functional cells. Changes in calcium were measured by converting the 340/380 ratio of Fura-2 florescence (after correction for background) as described. Data obtained from at least three independent experiments ($n = 20$ cells) were averaged and plotted (*B*). Representative NMDA currents activated by 50 μM NMDA plus 1 mM glycine and their inhibition by 100 and 1000 μM (−)-PA are shown in *C* and *D*, respectively. (−)-PA was first applied for 30 s and then simultaneously applied with NMDA. Membrane potential was clamped at 270 mV. *E* shows the (−)-PA concentration-response relationship for inhibition of NMDA currents activated by 50 μM NMDA plus 1 μM glycine. The concentration-response curve was fitted by the logistic equation with an IC_{50} value of 34.37 ± 0.012 μM and a Hill slope factor of 1.712 ± 0.038 ($n = 10$). Data in *E* represent the average of 10 neurons. *Error bars* represent the mean ± S.E. ** indicates $p < 0.05$ compared with NMDA group in *B* using one-way ANOVA with Tukey's post hoc analysis ($n = 20$). *Imemb*, total transmembrane ionic current.

metabolites were present in quantifiable amounts in the mouse food. Fourth, our results showed that in the ischemic brain (−)-PA levels significantly increased. Interestingly, the induction of (−)-PA in the ischemic brain was not followed by an increase of any other ABA metabolites, not even DPA, the downstream product of PA in the ABA catabolic pathway known in plants. This suggests that (−)-PA was either transported from elsewhere, such as the CSF, or the result of an alternate metabolic pathway different from that in plants. Therefore, the only plausible conclusion from these studies is that the high levels of (−)-PA seen in rodent brains could only be generated from endogenous sources. Indeed, double immunostaining and confocal fluorescence microscopy data lend further support to the argument that (−)-PA in the CSF was derived from the choroid plexus and brain endothelial cells.

What are the pathophysiological functions of brain (−)-PA? Cerebral ischemia initiates a complex cascade of biochemical events among which the excessive release of glutamate and its induction of excitotoxicity represent a major and early response in the brain (6). Overstimulation of NMDA receptors with glutamate results in an excessive influx of $[Ca^{2+}]_i$. Increased $[Ca^{2+}]_i$ activates a plethora of potentially neurotoxic mechanisms, such as the early induction of a calcium-dependent protease, calpain, which cleaves intracellular structural proteins such as spectrin, causing the collapse of intracellular structures and eventually neuronal death. Excitotoxicity contributes to a wide range of neurological disorders, such as stroke. Pharmacological inhibition of NMDARs ameliorates excitotoxicity-mediated neuronal death and protects the brain after cerebral ischemia (7). Given that ratiometric calcium imaging and whole-cell recording showed that (−)-PA dose-dependently blocks NMDA receptors, it has been determined that (−)-PA plays a key role in modulating NMDA receptors. The fact that (−)-PA is present in great quantities in both the viable brain tissues surrounding the ischemic core and the contralateral side of the brain strongly suggests that (−)-PA may play a role in protecting neurons. Indeed, injection of purified (−)-PA protected mouse brain against MCAO, whereas administering an antibody against (−)-PA exacerbated brain injury following MCAO. It is also intriguing as to why (−)-PA was present in the contralateral side of the brain. Based on immunostaining and MS analysis, a major site of (−)-PA production was traced to the choroid plexus. Rat CSF contains a very high level of (−)-PA. During ischemic reperfusion, increased (−)-PA may be circulated with CSF into both the

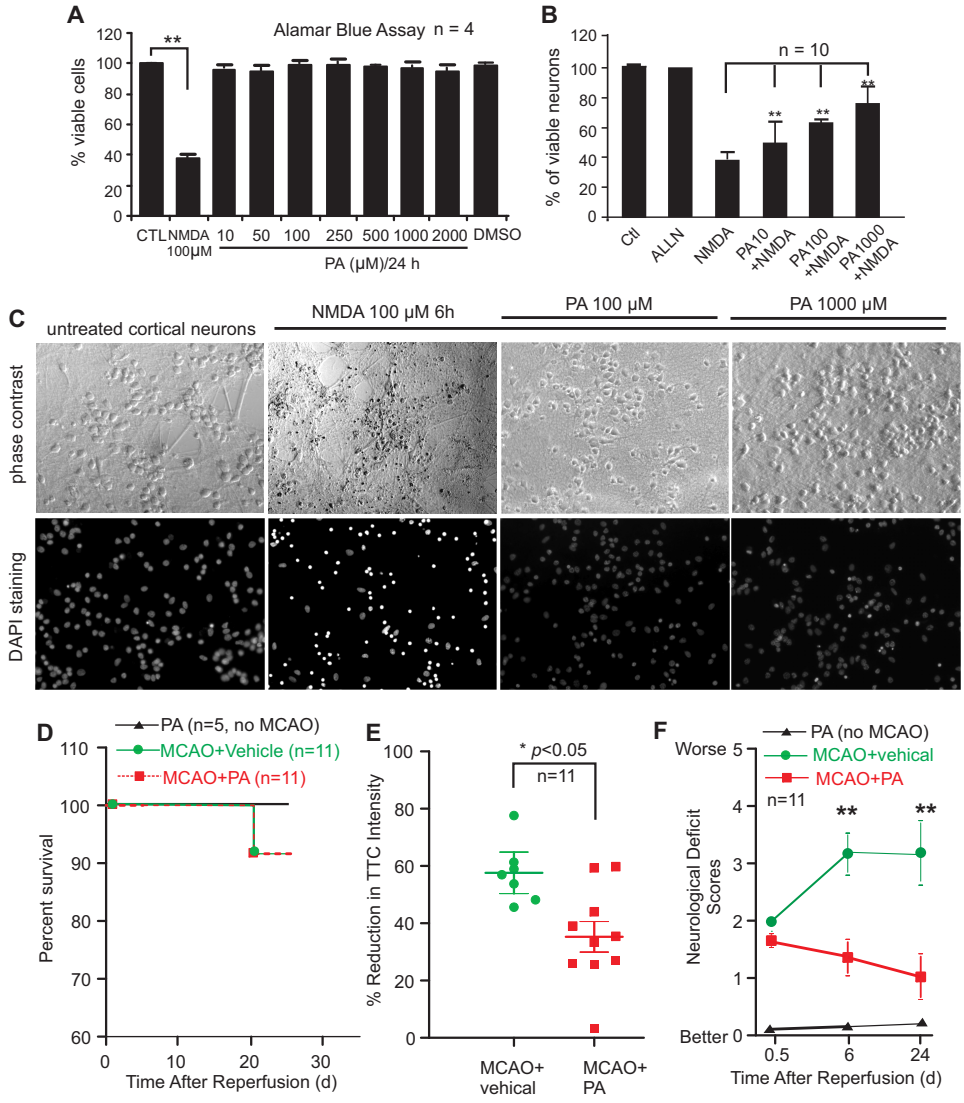

FIGURE 7. **(−)-PA protects cultured cortical neurons against glutamate toxicity and reduces ischemic brain injury.** Neuronal viability was assessed using the Alamar Blue assay. NMDA at 100 μM reduced cellular viability to 40% compared with the untreated control (*A*). (−)-PA alone has no toxicity to neurons (*A*). Adding (−)-PA to NMDA-treated neurons significantly protected cells from death (*B*). DAPI staining of cellular nuclei is shown in *C*. Data represent the mean ± S.E. ** indicates $p < 0.05$ (one-way ANOVA with Tukey's post hoc analysis; $n = 5$). *D–F*, (−)-PA protects mouse brain from MCAO-induced damage. Mice were subjected to 1 h of MCAO and 24 days of reperfusion as described under "Experimental Procedures." An osmotic pump was preimplanted before MCAO surgery to deliver (−)-PA into the ischemic side of the brain ventricle as described under "Experimental Procedures." (−)-PA was also delivered to non-MCAO mice, which served as a control. *D*, mouse survival rate was plotted. (−)-PA itself or administered into MCAO mice did not alter significantly the survival rate as this MCAO model has a very low mortality rate to begin with. Brain slices were stained with TTC, and soluble TTC was extracted and measured using a spectrophotometer (*E*). Quantification of TTC staining showed a significant reduction in brain infarction compared with the vehicle-treated mice (*E*; *, $p < 0.05$, paired *t* test; $n = 11$). Neurological deficit scores were also measured at 0.5 h, 6 days, and 24 days after MCAO and reperfusion (*F*). *Error bars* represents the mean ± S.D. ** indicates $p < 0.01$ by paired *t* test. *CTL*, control.

ipsilateral and contralateral sides of the brain, which explains the widespread presence of (−)-PA in the brain.

What are the potential implications of (−)-PA as an endogenous inhibitor against NMDA receptors? Agents that inhibit NMDA receptors in a transient and reversible manner are of significant interest for drug development against glutamate toxicity (9, 10), because these drugs uncompetitively inhibit NMDA receptor functions. These drugs do not interfere with the physiological functions of NMDA receptors. Our studies showed that (−)-PA has electrophysiological profiles in NMDA receptor inhibition similar to that of memantine, a gold standard in uncompetitive NMDAR inhibition. Although whether PA acts uncompetitively at NMDA receptors needs to be further demonstrated, it is highly possible that induction of (−)-PA by choroid plexus in response to cerebral ischemia represents an endogenous stress response in the brain. An increased level of (−)-PA outside of the ischemic core and the contralateral side of the brain tissue provides an endogenous defense mechanism for brain protection. These findings are novel and potentially important in developing (−)-PA and its analogous as neuroprotectants in the treatment of stroke.

Experimental Procedures

Materials—ABA metabolites standards DPA, ABA-GE, PA, 7′-OH-ABA, *neo*-PA, and *trans*-ABA were synthesized and prepared at the National Research Council of Canada, Saska-

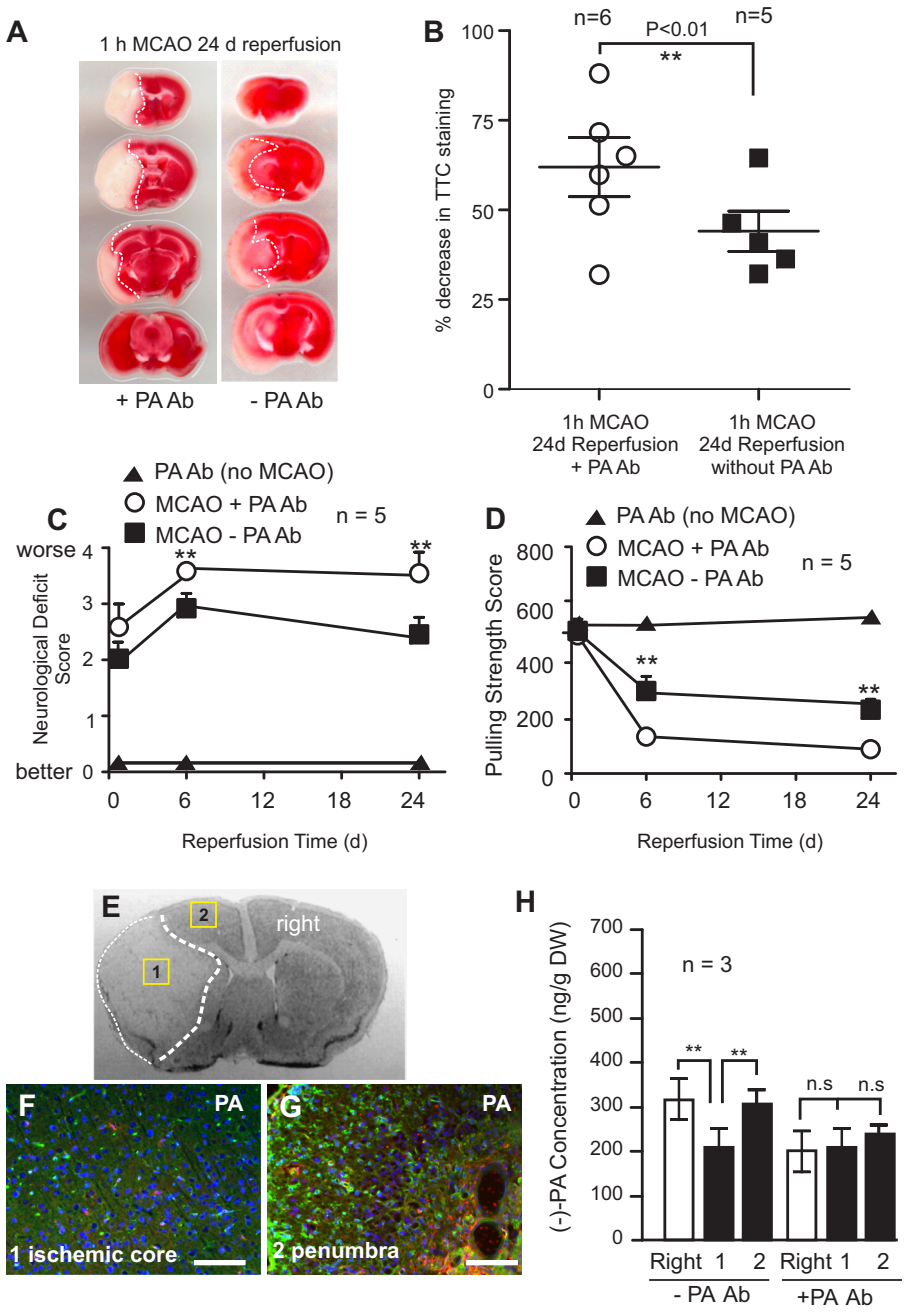

FIGURE 8. **Reduction of (−)-PA level exacerbates brain injury in MCAO mice.** Mice were subjected to 1 h of MCAO and 24 h of reperfusion as described under "Experimental Procedures." An osmotic pump was preimplanted before MCAO surgery to deliver PA monoclonal antibody into the ischemic side of the brain ventricle as described under "Experimental Procedures." TTC staining of brain slices is shown in *A*. The infarct areas are highlighted with *dotted lines* (*A*). The infarct volume at 24 h of reperfusion was quantified and is shown in *B*. Infusion of PA monoclonal antibody significantly increased infarct volume compared with vehicle (saline)-infused ischemic brain. The neurological deficit scores (*C*) and forepaw pulling strength (*D*) were also measured and compared among the three groups (▲, PA without MCAO; ○, PA Ab with MCAO; ■, no PA Ab with MCAO). *E*, a sample of ischemic brain coronal section highlighting areas of interests. Fluorescence double immunohistochemical staining of ischemic mouse brain infused with PA antibody showed reduced PA immunofluorescence (*red* color) both in the ischemic core (*F*) and the surrounding penumbra (*G*). Blood vessels were stained with lectin (*green* color). For comparison with a control group lacking PA antibody treatment, please see Fig. 5, *D*, *E*, and *F*. To confirm this, brain tissues were laser-microdissected out from *areas 1* and *2* and the contralateral side (labeled as *right*) for UPLC/MS/MS quantification of (−)-PA levels (*H*). The (−)-PA level was significantly reduced in the ischemic side of the brain surrounding the core. *Error bars* represent the mean ± S.D. ** indicates $p < 0.01$ by paired *t* test ($n = 5$). *n.s.*, non-significant with $p = 0.2$, one-way ANOVA with Tukey's post hoc analysis. *d*, days. *Scale bars*, 100 μm.

toon, Canada, and (±)-ABA was purchased from Sigma-Aldrich. Deuterated forms of the hormones used as internal standards included d_3-DPA, d_5-ABA-GE, d_3-PA, d_4-7′-OH-ABA, d_3-neoPA, d_4-ABA, and d_4-*trans*-ABA. These hormones were synthesized and prepared as published previously (19). The deuterated forms of the selected hormones used as recovery (external) standards were d_6-ABA and d_2-ABA-GE also prepared and synthesized at the National Research Council of Canada, Saskatoon. Antibodies and their conditions of usage are described in Table 1.

Animal Study Design—The clinical failure of many candidate drugs that showed promise in acute experimental cerebral

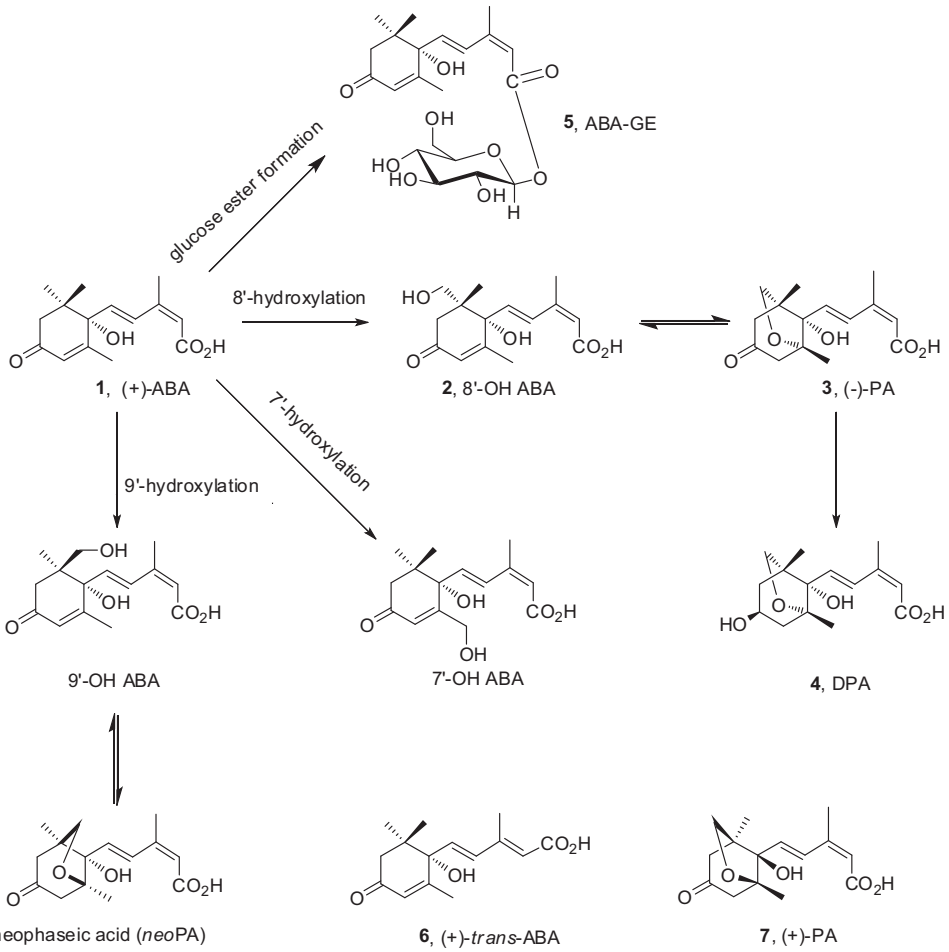

FIGURE 9. **Known metabolic pathways of (+)-ABA in plants.** The principal oxidative pathway of natural (+)-ABA (**1**), mediated by cytochrome P-450 monooxygenases, occurs through hydroxylation of the 8′-methyl group resulting in 8′-hydroxy-ABA (**2**), which rearranges to PA (**3**). Further enzymatic reduction of PA leads to DPA (**4**). Other metabolic steps include hydroxylation of the 7′- and 9′-methyl groups of the ABA ring as well as the conjugation of glucose esters (ABA-GE; **5**). In plants, *trans*-ABA (**6**) is a product of isomerization of natural ABA under UV light. The unnatural mirror image form of PA (**7**) may also occur as a result from the feeding of unnatural (−)-ABA.

ischemia underscores the importance of rigorous and comprehensive preclinical testing along published guidelines and recommendations by expert panels, including the Stroke Therapy Academic Industry Roundtable (STAIR) (20, 21) and Animal Research: Reporting *in Vivo* Experiments (ARRIVE) (22). Therefore, we randomized and concealed allocation to treatment groups, reported all mortality as well as attrition due to other causes, and analyzed the data according to the intention-to-treat principle and did not exclude animals showing signs of adverse effects, such as vomiting or aspiration. Multiple experimenters blinded to the treatment group performed surgeries, assessed end points, and administered all compounds as (−)-PA and other ABAs in solution cannot be distinguished from the vehicle by their colors.

Animal Surgery and MCAO—All procedures using animals were approved by the Human Health Therapeutics Animal Care Committee following the guidelines established by the Canadian Council on Animal Care. C57B/6 mice (20–23 g) were obtained from Charles River and bred locally. Under temporary isoflurane anesthesia, MCAO was induced by the intraluminal insertion of a silicon-coated nylon filament (Re L910 PK5, Doccol Corp.) through the common carotid artery into the internal carotid artery and left in place for 60 min as we described previously (23–29). Cerebral blood flow was monitored by laser Doppler flowmetry using a probe located in the ipsilateral parietal bone (1–2 mm posterior to bregma), and a >90% reduction in CSF was considered to indicate successful occlusion. The head temperatures were maintained at 37 °C using a warming lamp. Sham animals were generated by the insertion of a filament into the internal carotid artery that was immediately withdrawn.

After 1 h of MCAO, the filament was withdrawn, blood flow was restored to normal as monitored by laser Doppler flowmetry, and wounds were sutured. The body temperature of the experimental animal was monitored before and after the MCAO surgery using a rectal probe and was maintained at 37 °C using a heating pad and lamp. In preliminary experiments to verify a consistent stroke procedure, measurements of blood pressure, blood gases, and pH were also performed as described previously (30–32). Blood was collected from the facial vein and kept at −80 °C. Brains were removed after 2 h, 6 h, 24 h, 3 days, 7 days, and 28 days of reperfusion, and the right and left hemispheres were isolated. Brain and blood samples were rap-

TABLE 1
Antibodies and their conditions used for immunostaining
NA, not applicable.

Immunostaining					
Primary antibodies			Secondary antibodies		
Name	Supplier, catalog no.	Working dilution/species	Name	Supplier, catalog no.	Working dilution
IBA-1	Wako, 019-19741	1:200/rabbit	Anti-rabbit Alexa Fluor 488	Invitrogen, A11008	1:5000
GFAP	Abcam, 7260	1:250/rabbit	Anti-rabbit Alexa Fluor 488	Invitrogen, A11008	1:5000
NG2	Millipore, AB5320	1:100/rabbit	Anti-rabbit Alexa Fluor 488	Invitrogen, A11008	1:5000
NeuN	Abcam, 104225	1:500/rabbit	Anti-rabbit Alexa Fluor 488	Invitrogen, A11008	1:5000
PDGFRβ	Abcam, 32570	1:100/rabbit	Anti-rabbit Alexa Fluor 488	Invitrogen, A11008	1:5000
CD31	Abcam, 7388-50	1:100/rat	Anti-rat Alexa Fluor 488	Invitrogen, A21208	1:5000
TTR	Thermo Fisher, PA5-27220	1:100/rabbit	Anti-rabbit Alexa Fluor 488	Invitrogen, A11008	1:5000
Fluorescein-labeled lectin	Vector Laboratories, FL-1171	1:200	NA	NA	NA
PA	Gift from Prof. E. W. Weiler	1:50/mouse	Anti-mouse rhodamine	Invitrogen, A21208	1:5000
MAP2	Abcam, 32454	1:250/rabbit	Anti-rabbit Alexa Fluor 488	Invitrogen, A11008	1:5000

idly frozen in liquid nitrogen and stored at −80 °C until they were lyophilized.

Rat Focal MCAO—Male Sprague-Dawley rats (Charles River) between 350 and 375 g were kept on a 12-h light-dark cycle and group-housed in plastic cages. Rats were allowed free access to food and water. A total of 20 rats were used and randomly separated into sham and ischemia groups. Each rat was anesthetized with isoflurane followed by MCAO using procedures modified from those described previously (31, 32). A 1-cm incision was made midway between the left eye and the external auditory canal to expose the skull. The left middle cerebral artery was exposed through a 2-mm burr hole in the skull 2–3 mm rostral to the fusion of the zygomatic arch with the squamosal bone. A 1-mm Codman microaneurysm clip was applied to the vessel, and the wound was closed with suture material. A 1.5-cm incision was made in the ventral surface of the neck. The right and left common carotid arteries were isolated and ligated for 2 h using atraumatic clips. During the surgical procedure, the rat's body temperature was maintained between 37 and 37.5 °C. At the end of 2 h, the carotid clips were removed, the neck wound was closed, and the animal was returned to its cage and allowed to recover for 24 h. This procedure reduced regional cerebral blood flow to 15% of the basal level during the ischemic period and returned it to 95% of the basal level upon reperfusion. Body temperature was controlled to 37.5 ± 0.5 °C both during anesthesia and after recovery. At 24 h of reperfusion, the 1-mm Codman microaneurysm clip at the left middle cerebral artery was carefully removed, and the CSF and brain tissue were collected after euthanization of the rat. The brain was removed and sliced in a rat brain matrix. Brain slices were stained with TTC to confirm the ischemic injury (infarct) with edema subtracted. The rest of the brain tissue was transferred into Eppendorf tubes and frozen at −80 °C.

Infarct Size Measurement—Infarct size was measured by a colorimetric staining method using TTC as described previously (28). Briefly, brains were dissected out and cut into four 2-mm-thick coronal slices, which were stained with 5 ml of 2% TTC for 90 min at 37 °C. Afterward, the tissue was rinsed with saline and subsequently exposed to a mixture of ethanol: dimethyl sulfoxide (1:1), which was used to solubilize the formazan product. After 24-h incubation in the dark, the red solvent extracts were diluted 1:20 with fresh ethanol/Me_2SO solvent in three tubes and placed in cuvettes. Absorbance was measured at 485 nm in a spectrophotometer, and the values were averaged. Percent loss in brain TTC staining in the ischemic side of the brain was compared with the contralateral side of the brain of the same animal using the following equation: Percent loss = (1 − (Absorbance of ischemic hemisphere/Absorbance of contralateral hemisphere) × 100).

Neurological Deficit Scores—Both a six-point scale assessment and forelimb grip strength test were performed. (*a*) An expanded six-point scale turning behavior test was used exactly as described previously (24, 33). Briefly, behavioral assessments were carried out 30 min after MCAO when animals were fully awake after anesthesia. Assessments were made by an individual blinded to the treatment of the mice. The neurological deficits were scored as follows: 0, normal; 1, mild turning behavior with or without inconsistent curling when picked up by tail, 50% attempts to curl to the contralateral side; 2, mild consistent curling, 50% attempts to curl to contralateral side; 3, strong and immediate consistent curling, mouse holds curled position for more than 1–2 s, the nose of the mouse almost reaches the tail; 4, severe curling progressing into barreling, loss of walking or righting reflex; 5, comatose or moribund. At least eight mice per group were evaluated, and scores were averaged for statistical analysis. (*b*) Forelimb grip strength test was performed using the Grip Strength Meter from Columbus Instruments (MyNeurolab, St. Louis, MO), which measures muscle strength and neuromuscular integration relating to the grasping reflex in the forepaws. The peak preamplifier automatically stores the peak pull force and shows it on a liquid crystal display. For each animal, at least 10 measurements were taken at a specific time point, and the mean and S.E. were calculated.

Rat CSF Collection—Each rat was anesthetized with isoflurane, and the head was flexed downward at ~45° on a homemade device. A small midline incision was made beginning between the ears. A retractor was placed with the spring side pointing in the rostral direction. The separation of the superficial muscles exposed an underlying layer of muscles, which was easily separated along the midline by blunt dissection. The atlanto-occipital membrane in between the occipital bone and the upper cervical vertebra was exposed. A butterfly needle (25 gauge × 19 mm) connected to a 1-ml syringe was used. The needle was used to directly puncture into the cisterna magna, and the clear CSF sample (100–250 μl) was drawn into the

syringe until blood appeared (38). A hemostat was used to clamp the silicon tubing as soon as blood appeared in CSF. The tube was then cut using scissors from the clear part to avoid blood contamination. The clear CSF was transferred into an Eppendorf tube, and the sample was kept frozen at −80 °C for further analysis. Blood samples were collected by heart puncture. The rat was killed by decapitation under anesthesia.

Extraction of PA and ABA Metabolites from the Brain, Blood, CSF, and Mouse Food Samples—Freeze-dried tissue was homogenized using a multitube ball mill (Mini-BeadBeater-96, Biospec Products Inc., Bartlesville, OK) and about 50 mg (or less in the case of CSF) per sample was weighed out into individual Falcon tubes. An aliquot (100 μl) containing all internal standards (d_3-DPA, d_5-ABA-GE, d_3-PA, d_4-7′-OH-ABA, d_3-*neo*-PA, d_4-ABA, and d_4-*trans*-ABA, each at a concentration of 0.2 ng/μl dissolved in water:acetonitrile (1:1, v/v) with 0.5% glacial acetic acid), was added to each sample followed by the extraction solvent (3 ml of isopropanol:water:glacial acetic acid (80:19: 1, v/v)). For the blood and CSF samples, the aqueous component (600 μl of acidified water) of the extraction solvent was initially added followed by the combined internal standard aliquot and the organic solvent portion of the extraction solvent (2.4 ml of isopropanol with 0.5% glacial acetic acid). After shaking in the dark for 24 h at 4 °C, samples were centrifuged, and the supernatant was isolated and dried on a Büchi Syncore Polyvap (Büchi, Switzerland). Samples were reconstituted in 100 μl of methanol:glacial acetic acid (99:1, v/v) followed by 900 μl of aqueous 1% glacial acetic acid and then partitioned twice against 2 ml of hexane. After separation, the aqueous layer was isolated and dried as described above. Dry samples were redissolved in 100 μl of methanol:glacial acetic acid (99:1, v/v) followed by 900 μl of aqueous 1% glacial acetic acid. The reconstituted samples were passed through equilibrated Oasis HLB cartridges (Waters, Mississauga, Ontario, Canada), and the eluate (acetonitrile:water:glacial acetic acid, 30:69:1, v/v/v) was dried on a Labconco Centrivap concentrator (Labconco Corp., Kansas City, MO). An internal standard blank was prepared with 100 μl of the deuterated internal standard mixture. Two quality control (QC) standards were prepared by adding 100 and 30 μl, respectively, of a mixture containing the analytes of interest (DPA, ABA-GE, PA, 7′-OH-ABA, *neo*-PA, ABA, and *trans*-ABA), each at a concentration of 0.2 ng/μl, to 100 μl of the internal standard mixture. Finally, samples, blanks, and QCs were reconstituted in an aqueous solution of 40% methanol (v/v) containing 0.5% acetic acid and a 0.1 ng/μl concentration of each of the recovery standards (d_6-ABA and d_2-ABA-GE) and subjected to UPLC/electrospray ionization-MS/MS analysis and quantification, as described below.

Quantification of PA and ABA Metabolites by UPLC/MS/MS—Analysis of ABA and metabolites was carried out by UPLC/electrospray ionization-MS/MS utilizing a Waters ACQUITY UPLC® system equipped with a binary solvent delivery system, column, and sample manager coupled to a Waters Micromass Quattro Premier XE quadrupole tandem mass spectrometer via a Z-spray interface as described previously (1, 16, 17, 34, 35).

The analytical UPLC column used was an ACQUITY UPLC high strength silica (HSS) C_{18} (2.1 × 100 mm, 1.8 μm) with an ACQUITY HSS C_{18} VanGuard precolumn (2.1 × 5 mm, 1.8 μm). Mobile phase A contained 0.025% glacial acetic acid in HPLC-grade water, and mobile phase B contained 0.025% glacial acetic acid in HPLC-grade acetonitrile. Sample volumes of 10 μl were injected onto the column at a flow rate of 0.40 ml/min under initial conditions of 2% mobile phase B, which was maintained for 0.2 min, increased to 15% mobile phase B at 0.4 min, and then increased to 50% mobile phase B at 5 min and up to 100% by 5.5 min. Mobile phase B was maintained to 100% up to 6.2 min and then decreased to 2% after 6.5 min and held until 8 min for column equilibration before the next injection.

The mass spectrometer was set to collect data in multiple reaction monitoring mode controlled by MassLynx v4.1 (Waters). The analytes were ionized by negative ion electrospray using the following conditions: capillary potential, 1.75 kV; desolvation gas flow, 1100 liters/h; cone gas flow, 150 liters/h; and source and desolvation gas temperatures, 120 and 350 °C, respectively. The resulting chromatographic traces were quantified off-line by QuanLynx v4.1 software (Waters). Calibration curves were created for all compounds of interest. QCs were run along with the tissue samples.

Enantioseparation of (−)-PA from (+)-PA by UPLC/MS/MS—The enantioseparation of PA was conducted on the same UPLC/MS instrument as described above using the analytical chiral column Regis (*R*,*R*) Whelk-O 5/100 Kromasil (4.6 × 150 mm, 5 μm; REGIS Technologies, Inc.). Mobile phase A comprised 0.1% acetic acid in HPLC-grade water, and mobile phase B comprised 0.1% acetic acid in HPLC-grade methanol. Sample volumes of 15 μl were injected onto the column at a flow rate of 0.40 ml/min under initial conditions of 55% mobile phase B, which was maintained for 1 min and then increased to 90% mobile phase B after 18 min and up to 100% mobile phase B after 19 min. 100% mobile phase B was maintained until 20 min, then decreased to 55% by 21 min, and held constant until 25 min for column equilibration before the next injection. Under these chromatographic conditions, the retention time of synthetic standards of natural (−)-PA and unnatural mirror image form (+)-PA were 13.0 and 12.2 min, respectively.

Cortical Neuronal Cultures—Primary cortical neurons were prepared from embryonic E15–16 CD1 mice and cultured in Neurobasal medium supplemented with B-27 and N2 (Invitrogen) for 7–14 days as described previously (23, 27, 28). Neurons in these cultures are fully mature and are responsive to glutamate-induced excitotoxicity. Briefly, hemispheres were explanted and cleaned free of meninges. Mechanical and enzymatic dissociation in a 0.025% (w/v) trypsin solution for 25 min followed. A trypsin inhibitor was then added to block the enzyme, and 0.05% (w/v) DNase was added to remove DNA from dead cells. A series of trituration and mild centrifugation steps were included to disperse the neurons prior to resuspension in medium and to remove undissociated debris prior to plating. Cells were plated onto 24-well plates containing poly-L-lysine -coated coverslips at a density of 6 × 10^5 cells/well. Cultures in 100-mm dishes were seeded with 2 × 10^7 cells in 10 ml of culture medium. Cells were incubated at 37 °C.

Neuronal Viability Assay—After 7 days *in vitro*, cortical neurons were treated with ABA for 15 min prior to the addition of 100 μM NMDA at 37 °C. The plates were then incubated for up to 24 h at 37 °C. Untreated cells were also included as controls. At the end of the treatment period, cells were either fixed for staining or subjected to a neuronal viability assay using Alamar Blue (Invitrogen). Stained cells were examined under a fluorescence microscope (Axiovert 200M, Carl Zeiss, Thornwood, NY), and digital images were taken and analyzed using ImageJ software (http://rsbweb.nih.gov/ij/). The viability of cortical neurons treated with glutamate and with or without ABAs as mentioned was assayed using an Alamar Blue assay (Invitrogen). Briefly, a 1:10 dilution of Alamar Blue was added to cells for 1 h at 37 °C. The medium was removed and read in a 96-well plate using a plate reader with a λ_{Ex} of 530 nm and λ_{Em} of 590 nm. Triplicate readings were obtained per experiment with three independent repeats.

Ratiometric Measurement of $[Ca^{2+}]_i$ Using Fura-2—A ratiometric measurement of $[Ca^{2+}]_i$ was performed using Fura-2 AM (28, 36). Briefly, mouse cortical neurons at 7 days *in vitro* on glass coverslips were loaded with 5 μM Fura-2 AM (Molecular Probes, Eugene, OR) plus 0.02% Pluronic (Molecular Probes) for 30 min at 37 °C. After rinsing with PSS Mg^{2+}-free buffer containing 2 mM HEPES, pH 7.2, 140 mM NaCl, 5 mM KCl, 2.3 mM $CaCl_2$, and 10 mM glucose and stabilization in the same buffer for 5 min, Fura-2 intensities were measured using a Northern Eclipse Digital Ratio Image System (EMPIX, Mississauga, Ontario, Canada) with an Axiovert 200 camera and light source (Carl Zeiss). Fura-2 fluorescence was measured at 510-nm emission with 340/380-nm dual excitation selected by a DG-5 system (Sutter Instrument Co., Novato, CA). $[Ca^{2+}]_i$ concentration was represented by the ratio of florescence intensities between the two excitation wavelengths of R340/380 of Fura-2 after a correction for background. The R340/380 for 10 cells in one field of each coverslip was averaged. The basal level of $[Ca^{2+}]_i$ was recorded for 20 s followed by the application of inhibitors and ABAs. Glutamate (100 μM) was dissolved in PSS buffer and added to cortical neurons. $[Ca^{2+}]_i$ was recorded for 60–100 s. After washing with PSS buffer for 300 s, PSS buffer containing 45 mM KCl was added to neurons to record changes in $[Ca^{2+}]_i$ for 60 s to show the viability of the neurons. All measurements were repeated at least three times. The data were analyzed using Microsoft Excel and presented as the mean of three experiments.

Whole-cell Electrophysiological Recordings—Whole-cell patch clamp recordings were carried out at room temperature (22–25 °C) using an Axopatch 700A patch clamp amplifier (Axon Instruments, Inverurie, Scotland). Data acquisition was achieved using a DigiData 1322A with pClamp 9.0 software. The acquisition rate was 10 kHz, and signals were filtered at 5 kHz. Patch electrodes were pulled with a Flaming/Brown micropipette puller (Sutter Instruments Co.) and fire-polished. The recording electrodes had a resistance of 4–6 megaohms when filled with different internal solutions. For the voltage clamp recordings, the capacity transients were cancelled using the resistance capacitance circuit within the amplifier. After the formation of whole-cell configuration, access resistances were generally <15 megaohms. Series resistance compensation was set to 70–90%. The liquid junction potential was ~2 mV and was autoadjusted each time by pipette offset. To record NMDA/AMPA-activated currents, an external solution containing 150 mM NaCl, 5 mM KCl, 0.2 mM $CaCl_2$, 10 mM glucose, and 10 mM HEPES, pH adjusted to 7.4 with NaOH, and a pipette solution containing 140 mM KCl, 2.5 mM $MgCl_2$, 10 mM HEPES, 11 mM EGTA, and 5 mM ATP, pH adjusted to 7.3 with KOH, were used. For voltage clamp recordings, the membrane potential was held at −70 mV unless noted otherwise. Drug solutions were prepared in extracellular solution and applied to neurons by pressure using the 8-Channel Focal Perfusion System (ALA Scientific Instruments, Farmingdale, NY). Neurons were bathed constantly in extracellular solution between drug applications. Drug solution exchange was accomplished by electronic control.

Patch clamp data were processed using Clampfit 9.0 (Axon Instruments) and then analyzed in Origin 7.5 (OriginLab, Northampton, MA). The dose-response curve was fitted to the following logistic equation: $y = (A_1 - A_2)/[1 + (x/x_0)p] + A_2$ where y is the response; A_1 and A_2 are the maximum and minimum responses, respectively; x_0 is the concentration corresponding to half-maximal effect; x is the drug concentration, and p is the Hill coefficient.

Indirect Immunofluorescence Staining and Confocal Microscopy—The procedures for indirect immunofluorescence immunocytochemistry were exactly as described previously (23, 25). Mouse monoclonal antibody to PA was a kind gift from Prof. E. W. Weiler (Department of Plant Physiology, Ruhr University Bochum, Bochum, Germany) as described previously (15, 37). The antibody to PA was diluted with distilled water to 0.2 mg/ml and used at a 1:50 dilution. The primary antibody was incubated with the tissue section in a humidified chamber overnight at 4 °C. Sections were then washed three times with 10 mM PBS for 10 min and incubated with a rhodamine-conjugated secondary antibody (Invitrogen) at a concentration of 1:5000 diluted in antibody buffer for 1 h at room temperature. For double immunostaining, after washing with PBS, primary antibodies to CD31, IBA-1, MAP2, GFAP, and NeuN (see Table 1) were incubated with the section at room temperature for 1 h. Fluorescein-conjugated anti-rabbit or -goat secondary antibody against these marker proteins (listed in Table 1) were incubated with the section for 1 h at room temperature.

Sections were then washed three times in 10 mM PBS for 10 min, and mounted with Dako fluorescent mounting medium spiked with 2 μg/ml Hoechst 33258 (Sigma) to counterstain nuclei. For some sections, the primary antibody incubation was omitted as a negative control. Confocal imaging was carried out on an Olympus Fluoview FV1000 confocal laser scanning microscope (Olympus, Markham, Ontario, Canada). Imaging was performed with a 20× or 40× objective.

Tissue Laser Capture Microdissection—Laser capture microdissection was conducted with a Leica LMD6 laser microdissection System (Leica Microsystems) using 10 infrared and two ultraviolet pulses. Areas of interests were dissected successively from the same brain slide, and all cells from the same region were pooled in a single laser capture microdissection colleting tube. Cells were lysed immediately after dissection and stored at −20 °C before UPLC/MS/MS analysis.

Infusion of (−)-PA and (−)-PA Antibody into the Brain Ventricles—Minipumps, with an infusion rate of 1.0 μl/h and a reservoir with up to 3-day delivery capacity (Alzet 1003D) (DURECT Corp., ALZET Osmotic Pumps, Cupertino, CA) were loaded with (−)-PA (50 mg/ml) or 100% saline (placebo) as described (38). The pumps were submerged in 0.9% sterile saline solution at 37 °C overnight to prime them so that (−)-PA was delivered immediately after implantation. Minipumps were preimplanted subcutaneously in the back immediately before the MCAO surgery.

Data Analysis—Data were analyzed using Microsoft Excel and GraphPad Prism 5.0. Statistical significance was determined either by a paired t test or by one-way ANOVA. The significant group was determined using a post hoc Tukey's test. $p < 0.05$ was considered statistically significant.

Author Contributions—S. X. J. performed animal brain tissue, blood, and CSF collections; preparation of these samples for analysis; TTC staining; infarct quantification; hypothermia treatment; and behavioral analysis. J. S. performed rat and mouse MCAO. X. H. performed UPLC/MS/MS analysis. L. I. Z. performed data analysis and result interpretation. C. L. B. provided some data analysis and discussion. S. T. H. and S. R. A. conceived the idea, provided financial support to the project, discussed the data, and analyzed the results. S. T. H. wrote the paper.

Acknowledgments—We thank the National Research Council of Canada animal facility for the timely supply of animals. We are especially grateful to Prof. E. W. Weiler and K. Hagemann (Department of Plant Physiology, Ruhr University Bochum) for the generous gift of PA antibody. We also thank Amy Aylsworth for meticulously proofreading the draft manuscript and Vera Cekic and Monika Lafond for technical assistance with hormone profiling sample preparation. Animal antibody work was assisted by Lu Zhang and Yancheng Tang. Patch clamping work was assisted by Lifeng Zheng, Mei Yu, and Dr. Ying Wang.

References

1. Krochko, J. E., Abrams, G. D., Loewen, M. K., Abrams, S. R., and Cutler, A. J. (1998) (+)-Abscisic acid 8′-hydroxylase is a cytochrome P450 monooxygenase. *Plant Physiol.* **118,** 849–860
2. Desikan, R., Cheung, M. K., Bright, J., Henson, D., Hancock, J. T., and Neill, S. J. (2004) ABA, hydrogen peroxide and nitric oxide signalling in stomatal guard cells. *J. Exp. Bot.* **55,** 205–212
3. Israelsson, M., Siegel, R. S., Young, J., Hashimoto, M., Iba, K., and Schroeder, J. I. (2006) Guard cell ABA and CO_2 signaling network updates and Ca^{2+} sensor priming hypothesis. *Curr. Opin. Plant Biol.* **9,** 654–663
4. White, P. J. (2000) Calcium channels in higher plants. *Biochim. Biophys. Acta* **1465,** 171–189
5. Seiler, C., Harshavardhan, V. T., Rajesh, K., Reddy, P. S., Strickert, M., Rolletschek, H., Scholz, U., Wobus, U., and Sreenivasulu, N. (2011) ABA biosynthesis and degradation contributing to ABA homeostasis during barley seed development under control and terminal drought-stress conditions. *J. Exp. Bot.* **62,** 2615–2632
6. Hou, S. T., and MacManus, J. P. (2002) Molecular mechanisms of cerebral ischemia-induced neuronal death. *Int. Rev. Cytol.* **221,** 93–148
7. Moskowitz, M. A., Lo, E. H., and Iadecola, C. (2010) The science of stroke: mechanisms in search of treatments. *Neuron* **67,** 181–198
8. Papadakis, M., Hadley, G., Xilouri, M., Hoyte, L. C., Nagel, S., McMenamin, M. M., Tsaknakis, G., Watt, S. M., Drakesmith, C. W., Chen, R., Wood, M. J., Zhao, Z., Kessler, B., Vekrellis, K., and Buchan, A. M. (2013) Tsc1 (hamartin) confers neuroprotection against ischemia by inducing autophagy. *Nat. Med.* **19,** 351–357
9. Lipton, S. A. (2006) Paradigm shift in neuroprotection by NMDA receptor blockade: memantine and beyond. *Nat. Rev. Drug Discov.* **5,** 160–170
10. Lipton, S. A. (2007) Pathologically activated therapeutics for neuroprotection. *Nat. Rev. Neurosci.* **8,** 803–808
11. Brandt, B., Munemasa, S., Wang, C., Nguyen, D., Yong, T., Yang, P. G., Poretsky, E., Belknap, T. F., Waadt, R., Alemán, F., and Schroeder, J. I. (2015) Calcium specificity signaling mechanisms in abscisic acid signal transduction in *Arabidopsis* guard cells. *Elife* **4,** e03599
12. Diaz, M., Sanchez-Barrena, M. J., Gonzalez-Rubio, J. M., Rodriguez, L., Fernandez, D., Antoni, R., Yunta, C., Belda-Palazon, B., Gonzalez-Guzman, M., Peirats-Llobet, M., Menendez, M., Boskovic, J., Marquez, J. A., Rodriguez, P. L., and Albert, A. (2016) Calcium-dependent oligomerization of CAR proteins at cell membrane modulates ABA signaling. *Proc. Natl. Acad. Sci. U.S.A.* **113,** E396–E405
13. Edel, K. H., and Kudla, J. (2016) Integration of calcium and ABA signaling. *Curr. Opin. Plant Biol.* **33,** 83–91
14. Le Page-Degivry, M. T., Bidard, J. N., Rouvier, E., Bulard, C., and Lazdunski, M. (1986) Presence of abscisic acid, a phytohormone, in the mammalian brain. *Proc. Natl. Acad. Sci. U.S.A.* **83,** 1155–1158
15. Gergs, U., Hagemann, K., Zeevaart, J. A. D., and Weiler, E. W. (1993) The determination of phaseic acid by monoclonal antibody-based enzyme immunoassay. *Bot. Acta* **106,** 404–410
16. Zaharia, L. I., Galka, M. M., Ambrose, S. J., and Abrams, S. R. (2005) Preparation of deuterated abscisic acid metabolites for use in mass spectrometry and feeding studies. *J. Label. Cmpd. Radiopharm.* **48,** 438–445
17. Zaharia, L. I., Walker-Simmon, M. K., Rodriguez, C. N., and Abrams, S. R. (2005) Chemistry of abscisic acid, abscisic acid catabolites and analogs. *J. Plant Growth. Regul.* **24,** 274–284
18. Balsevich, J. J., Cutler, A. J., Lamb, N., Friesen, L. J., Kurz, E. U., Perras, M. R., and Abrams, S. R. (1994) Response of cultured maize cells to (+)-abscisic acid, (−)-abscisic acid, and their metabolites. *Plant Physiol.* **106,** 135–142
19. Abrams, S. R., Nelson, K., and Ambrose, S. J. (2013) Deuterated abscisic acid analogs for mass spectrometry and metabolism studies. *J. Label. Compd. Radiopharm.* **46,** 273–283
20. Fisher, M., Feuerstein, G., Howells, D. W., Hurn, P. D., Kent, T. A., Savitz, S. I., Lo, E. H., and STAIR Group (2009) Update of the stroke therapy academic industry roundtable preclinical recommendations. *Stroke* **40,** 2244–2250
21. Saver, J. L., Albers, G. W., Dunn, B., Johnston, K. C., Fisher, M., and STAIR VI Consortium (2009) Stroke Therapy Academic Industry Roundtable (STAIR) recommendations for extended window acute stroke therapy trials. *Stroke* **40,** 2594–2600
22. Kilkenny, C., Browne, W., Cuthill, I. C., Emerson, M., Altman, D. G., National Centre for the Replacement, R., and National Centre for the Replacement, Refinement and Reduction of Animals in Research (2011) Animal research: reporting *in vivo* experiments—the ARRIVE guidelines. *J. Cereb. Blood Flow Metab.* **31,** 991–993
23. Hou, S. T., Jiang, S. X., Desbois, A., Huang, D., Kelly, J., Tessier, L., Karchewski, L., and Kappler, J. (2006) Calpain-cleaved collapsin response mediator protein-3 induces neuronal death after glutamate toxicity and cerebral ischemia. *J. Neurosci.* **26,** 2241–2249
24. Hou, S. T., Keklikian, A., Slinn, J., O'Hare, M., Jiang, S. X., and Aylsworth, A. (2008) Sustained up-regulation of semaphorin 3A, neuropilin1, and doublecortin expression in ischemic mouse brain during long-term recovery. *Biochem. Biophys. Res. Commun.* **367,** 109–115
25. Hou, S. T., Jiang, S. X., Aylsworth, A., Ferguson, G., Slinn, J., Hu, H., Leung, T., Kappler, J., and Kaibuchi, K. (2009) CaMKII phosphorylates collapsin response mediator protein 2 and modulates axonal damage during glutamate excitotoxicity. *J. Neurochem.* **111,** 870–881
26. Hou, S. T., Jiang, S. X., Slinn, J., O'Hare, M., and Karchewski, L. (2010) Neuropilin 2 deficiency does not affect cortical neuronal viability in response to oxygen-glucose-deprivation and transient middle cerebral artery occlusion. *Neurosci. Res.* **66,** 396–401

27. Hou, S. T., Jiang, S. X., Aylsworth, A., Cooke, M., and Zhou, L. (2013) Collapsin response mediator protein 3 deacetylates histone H4 to mediate nuclear condensation and neuronal death. *Sci. Rep.* **3,** 1350
28. Jiang, S. X., Lertvorachon, J., Hou, S. T., Konishi, Y., Webster, J., Mealing, G., Brunette, E., Tauskela, J., and Preston, E. (2005) Chlortetracycline and demeclocycline inhibit calpains and protect mouse neurons against glutamate toxicity and cerebral ischemia. *J. Biol. Chem.* **280,** 33811–33818
29. Jiang, S. X., Kappler, J., Zurakowski, B., Desbois, A., Aylsworth, A., and Hou, S. T. (2007) Calpain cleavage of collapsin response mediator proteins in ischemic mouse brain. *Eur. J. Neurosci.* **26,** 801–809
30. MacManus, J. P., Hill, I. E., Huang, Z. G., Rasquinha, I., Xue, D., and Buchan, A. M. (1994) DNA damage consistent with apoptosis in transient focal ischaemic neocortex. *Neuroreport* **5,** 493–496
31. MacManus, J. P., Buchan, A. M., Hill, I. E., Rasquinha, I., and Preston, E. (1993) Global ischemia can cause DNA fragmentation indicative of apoptosis in rat brain. *Neurosci. Lett.* **164,** 89–92
32. Tu, Y., Hou, S. T., Huang, Z., Robertson, G. S., and MacManus, J. P. (1998) Increased Mdm2 expression in rat brain after transient middle cerebral artery occlusion. *J. Cereb. Blood Flow Metab.* **18,** 658–669
33. Jiang, S. X., Sheldrick, M., Desbois, A., Slinn, J., and Hou, S. T. (2007) Neuropilin-1 is a direct target of the transcription factor E2F1 during cerebral ischemia-induced neuronal death *in vivo*. *Mol. Cell. Biol.* **27,** 1696–1705
34. Ross, A. R., Ambrose, S. J., Cutler, A. J., Feurtado, J. A., Kermode, A. R., Nelson, K., Zhou, R., and Abrams, S. R. (2004) Determination of endogenous and supplied deuterated abscisic acid in plant tissues by high-performance liquid chromatography-electrospray ionization tandem mass spectrometry with multiple reaction monitoring. *Anal. Biochem.* **329,** 324–333
35. Zaharia, L. I., Gai, Y., Nelson, K. M., Ambrose, S. J., and Abrams, S. R. (2004) Oxidation of 8′-hydroxy abscisic acid in Black Mexican Sweet maize cell suspension cultures. *Phytochemistry* **65,** 3199–3209
36. Jiang, S. X., Benson, C. L., Zaharia, L. I., Abrams, S. R., and Hou, S. T. (2010) Abscisic acid does not evoke calcium influx in murine primary microglia and immortalised murine microglial BV-2 and N9 cells. *Biochem. Biophys. Res. Commun.* **401,** 435–439
37. Eberle, J., Arnscheidt, A., Klix, D., and Weiler, E. W. (1986) Monoclonal antibodies to plant growth regulators: III. zeatinriboside and dihydrozeatinriboside. *Plant Physiol.* **81,** 516–521
38. DeVos, S. L., and Miller, T. M. (2013) Direct intraventricular delivery of drugs to the rodent central nervous system. *J. Vis. Exp.* e50326